Theoretical and Experimental Studies of Thermodynamic Properties, Anharmonic Effects and Structural Determination of HCP Crystals

Dinh Quoc Vuong[1] and Nguyen Van Hung[2,*]

[1]*Cam Pha School, Quang Ninh Education & Training Department. Nguyen Van Cu, Ha Long, Quang Ninh, Vietnam*

[2]*Department of Physics, Hanoi University of Science. 334 Nguyen Trai, Thanh Xuan, Hanoi, Vietnam*

Abstract: Thermodynamic properties, anharmonic effects and structural determination of hcp crystals have been studied based on their theoretical and experimental Debye-Waller factor presented in terms of cumulant expansion up to the third order in X-ray absorption fine structure (XAFS). The results have been achieved based on the present advanced method using that the calculations and measurements are necessary only for the second cumulants from which all the considered XAFS quantities have been provided. This advantage has resulted based on the description of XAFS quantities in terms of second cumulants. The many-body effects included in the present one-dimensional model have been taken into account based on the first shell near neighbor contributions to the vibration between absorber and backscaterer atoms. Morse potential is assumed to describe the single-pair atomic interaction included in the anharmonic interatomic effective potential. Numerical and experimental results for Zn in hcp phase obtained by the present advanced method are found to be in good agreement with one another and with those measured at HASYLAB (DESY, Germany).

Keywords: Thermodynamic properties, Structural parameter, XAFS, Debye-Waller factor, Hcp crystals.

1. INTRODUCTION

X-ray Absorption Fine Structure (XAFS) has developed into a powerful technique for providing information on the local atomic structure and thermodynamic properties of substances. The formalism for including anharmonic effects in XAFS is often based on cumulant expansion approach [1] from which the anharmonic XAFS function has resulted as

$$\chi(k) = F(k)\frac{e^{-2R/\lambda(k)}}{kR^2}\mathrm{Im}\left\{e^{i\Phi(k)}\exp\left[2ikR+\sum_n \frac{(2ik)^n}{n!}\sigma^{(n)}\right]\right\}, \quad (1)$$

where F(k) is the real atomic backscattering amplitude, *k* and λ are the wave number and mean free path of photoelectron, respectively, Φ is the net phase shift, $R = \langle r \rangle$ with *r* being the instantaneous bond length between absorber and backscatterer atoms, and $\sigma^{(n)}$ (n = 1, 2, 3,…) are the cumulants describing Debye-Waller factor (DWF).

Hence, the precise DWFs or cumulants are crucial to quantitative treatment of XAFS spectra where the even cumulants contribute to the amplitude, the odd ones to the phase of XAFS spectra [2]. These cumulants describe the thermodynamic properties and anharmonic effects of substances. Consequently, the lack of the precise cumulants has been one of the biggest limitations to accurate structural determinations (*e.g.*, the coordination numbers and the atomic distances) [3] and to specify the thermodynamic properties of substances [3-9] from XAFS. Therefore, investigation of XAFS cumulants is of great interest.

The purpose of this work is to study the thermodynamic properties, anharmonic effects and structural parameters of hcp (hexagonal closed packed) crystals based on their theoretical and experimental cumulants, thermal expansion coefficients, XAFS spectra and their Fourier transform magnitudes. The results have been achieved based on the present advanced method using that the calculations and measurements are necessary only for the second cumulants or mean square relative displacement (MSRD) from which all the considered quantities have been provided. This advanced method has resulted (Section 2) based on the description of the analytical expressions for the considered XAFS quantities derived using the anharmonic correlated Einstein model (ACEM) [9] in terms of second cumulants. The many-body effects included in the present one-dimensional model are taken into account based on the first shell near neighbor contributions approach (FSNNCA) to the vibration between absorber and backscatterer atoms. Morse potential is assumed to describe the single-pair atomic interaction included

*Address correspondence to this author at the Department of Physics, Hanoi University of Science, 334 Nguyen Trai, Thanh Xuan, Hanoi, Vietnam;
E-mail: hungnv@vnu.edu.vn

E-ISSN: 2408-977X/17

in the anharmonic interatomic effective potential. The present advanced method has also been applied to extracting the experimental XAFS parameters of Zn based on the experimental values of its second cumulants measured at the Beamline BL8, Synchrotron Light Research Institute (SLRI), Thailand. Numerical results for Zn (Section 3) are compared to the experimental values extracted by using this advanced method and to those measured at HASYLAB (DESY, Germany) [10] which show good agreement. The conclusions on the obtained results are presented in Section 4.

2. CUMULANTS, THERMAL EXPANSION COEFFICIENT AND XAFS OF HCP CRYSTALS

2.1. Theory

In order to include anharmonic effects, the Hamiltonian of system in the present theory contains the anharmonic interatomic effective potential expressed as

$$V_{eff}(x) \approx \frac{1}{2} k_{eff} x^2 + k_{3eff} x^3, \; x = r - r_0, \tag{2}$$

where k_{eff} is the effective local force constant and k_{3eff} is the cubic anharmonic parameter giving an asymmetry of the anharmonic effective potential, *r* and r_0 are the instantaneous and equilibrium distances between absorber and backscatterer atoms, respectively.

Using the FSNNCA which was successfully applied to bcc (body centered cubic) crystals [8], the anharmonic effective potential for hcp crystals has the form

$$V_{eff}(x) = V(x) + \sum_{i=1,2} \sum_{j \neq i} V\left(\frac{1}{2} x \hat{\boldsymbol{R}}_{12} \cdot \hat{\boldsymbol{R}}_{ij} \right), \tag{3}$$

where $\hat{\boldsymbol{R}}$ is unit vector; the sum *i* is over absorber (*i* = 1) and backscatterer (*i* = 2), and the sum *j* is over all their first shell near neighbors, excluding the absorber and backscatterer themselves, whose contributions are included in the term *V*(*x*).

The Morse potential expanded up to the third order around its minimum

$$V(x) = D\left(e^{-2\alpha x} - 2e^{-\alpha x} \right) \approx D\left(-1 + \alpha^2 x^2 - \alpha^3 x^3 \right) \tag{4}$$

is assumed to describe the single-pair atomic interaction included in the anharmonic effective potential where α describes the width of the potential and D is the dissociation energy. Therefore, substituting this Morse potential into Eq. (3) and comparing the results to Eq. (2) the values of k_{eff}, k_{3eff} in terms of Morse parameters for hcp crystals included in all XAFS cumulants expressions are determined.

Using further the definition $y = x - a, \; a = \langle x \rangle$ [9] the anharmonic interatomic effective potential Eq. (3) for hcp crystals is described in the summation of the harmonic contribution and a perturbation δV as

$$V_{eff}(y) = \frac{5}{2} D\alpha^2 y^2 + \delta V(y), \; \delta V \cong 5D\alpha^2 \left(a - \frac{1}{4} \alpha y^2 \right) y. \tag{5}$$

The derivation of XAFS cumulants for hcp crystals in this work is based on the quantum statistical theory [11] and the parameters of the anharmonic interatomic effective potentials given by Eqs. (2) - (5), as well as an averaging procedure using the canonical partition function Z and statistical density matrix ρ, *e.g.*,

$$\langle y^m \rangle = \frac{1}{Z} Tr\left(\rho y^m \right), \quad m = 1, 2, 3, \cdots \tag{6}$$

Atomic vibrations are quantized in terms of phonons, and anharmonicity is the result of phonon-phonon interaction, that is why we express y in terms of the annihilation and creation operators, $\hat{a}$ and $\hat{a}^+$, respectively

$$y \equiv a_0 \left(\hat{a} + \hat{a}^+ \right), \; a_0 = \sqrt{\frac{\hbar \omega_E}{10 D\alpha^2}}, \tag{7}$$

which have the following properties

$$\begin{aligned} &\left[\hat{a}, \hat{a}^+ \right] = 1, \; \hat{a}^+ |n\rangle = \sqrt{n+1} |n+1\rangle, \\ &\hat{a} |n\rangle = \sqrt{n-1} |n-1\rangle, \; \hat{a}^+ \hat{a} |n\rangle = n |n\rangle, \end{aligned} \tag{8}$$

as well as use the harmonic oscillator state $|n\rangle$ as the eigenstate with the eigenvalue $E_n = n\hbar\omega_E$ for *n* being the phonon number, ignoring the zero-point energy for convenience.

Due to weak anharmonicity in XAFS, the canonical partition function included in Eq. (6) can be expressed as

$$Z \cong Z_0 = \sum_n e^{-n\beta\hbar\omega_E} = \sum_{n=0}^{\infty} z^n = \frac{1}{1-z}, \; z = \exp\left(-\theta_E / T \right). \tag{9}$$

Here, the correlated Einstein frequency ω_E and temperature θ_E for hcp crystals have the forms

$$\omega_E = \sqrt{\frac{10D\alpha^2}{M}},\ \theta_E = \frac{\hbar\omega_E}{k_B}, \tag{10}$$

where M is the atomic mass and k_B is Boltzmann constant.

Using the above results for the correlated atomic vibration and the procedure depicted by Eqs. (6) - (10), as well as the first-order thermodynamic perturbation theory [11], the temperature-dependent XAFS cumulants have been derived.

Here, based on the procedure depicted by Eqs. (6) – (10) we derived the even moment expressing the second cumulant or MSRD

$$\sigma^2(T) = \left\langle y^2 \right\rangle = \sum_n e^{-n\beta\hbar\omega_E} \left\langle n|y^2|n\right\rangle,\ \beta = 1/k_BT \tag{11}$$

and the odd moments expressing the first (m = 1) and third (m = 3) cumulants

$$\sigma^{(1)}(T) = a = \sigma_0^{(1)}\frac{1+z(T)}{1-z(T)} = \frac{\sigma_0^{(1)}}{\sigma_0^2}\sigma^2(T),\ \sigma_0^{(1)} = \frac{3\alpha}{4}\sigma_0^2\ , \tag{12}$$

where the operations expressed by Eqs. (8) have been applied to calculate the matrix elements given in Eqs. (11) and (12).

Consequently, the XAFS expressions have resulted for the second cumulant or MSRD

$$\sigma^2(T) = \left\langle y^2 \right\rangle = \sigma_0^2\frac{1+z(T)}{1-z(T)},\ \sigma_0^2 = \frac{\hbar\omega_E}{10D\alpha^2}, \tag{13}$$

for the first cumulant or net thermal expansion

$$\sigma^{(1)}(T) = a = \sigma_0^{(1)}\frac{1+z(T)}{1-z(T)} = \frac{\sigma_0^{(1)}}{\sigma_0^2}\sigma^2(T),\ \sigma_0^{(1)} = \frac{3\alpha}{4}\sigma_0^2\ , \tag{14}$$

and for the third cumulant or mean cubic relative displacement (MCRD)

$$\sigma^{(3)}(T) = \left\langle y^3 \right\rangle = \sigma_0^{(3)}\left[3\left(\frac{\sigma^2(T)}{\sigma_0^2}\right)^2 - 2\right],\ \sigma_0^{(3)} = \frac{\alpha}{2}\left(\sigma_0^2\right)^2\ . \tag{15}$$

Further, using the first cumulant given by Eq. (14), the expression for the thermal expansion coefficient has been derived and given by

$$\alpha_T(T) = \frac{1}{r}\frac{da}{dT} = \alpha_T^0\frac{\left(\sigma^2(T)\right)^2 - \left(\sigma_0^2\right)^2}{T^2},\ \alpha_T^0 = \frac{15D\alpha^3}{4k_Br}\ . \tag{16}$$

In the above expressions, $\sigma_0^{(1)}$, σ_0^2, $\sigma_0^{(3)}$ in the above expressions are zero-point energy contributions to three first XAFS cumulants $\sigma^{(1)}(T)$, $\sigma^2(T)$, $\sigma^{(3)}(T)$, respectively, and α_T^0 is the constant value which the thermal expansion coefficient approaches at high-temperatures.

Moreover, the second cumulant given by Eq. (13) is harmonic while the experimental data always include the temperature-dependent anharmonic effects. That is why we introduce the total second cumulant or MSRD as

$$\sigma_{tot}^2(T) = \sigma^2(T) + \sigma_A^2(T), \tag{17}$$

which involves an anharmonic contribution

$$\sigma_A^2(T) = \beta_A(T)\left[\sigma^2(T) - \sigma_0^2\right], \tag{18}$$

containing the anharmonic factor

$$\beta_A(T) = \frac{9\alpha^2}{8}\sigma^2(T)\left[1 + \frac{3\alpha}{4R}\sigma^2(T)\left(1 + \frac{3\alpha}{4R}\sigma^2(T)\right)\right]. \tag{19}$$

Further, for structural determination using the above obtained cumulants the k-edge XAFS function [14] has resulted for hcp crystals

$$\chi(k,T) = \sum_j \frac{S_0^2 N_j}{kR_j^2}F_j(k)F_A(k,T)e^{-\left(2k^2\sigma^2(T)+2R_j/\lambda(k)\right)}\sin\left(2kR_j + \Phi_j(k) + \Phi_A^j(k,T)\right), \tag{20}$$

which contains the anharmonic contribution to amplitude described by the factor

$$F_A(k,T) = \exp\left[-2k^2\sigma_A^2(T)\right], \tag{21}$$

causing the anharmonic attenuation and the anharmonic contribution to phase

$$\Phi_A^j(k,T) = 2k\left[\sigma^{(1)}(T) - 2\sigma_A^2(T)\left(\frac{1}{R_j} - \frac{1}{\lambda(k)}\right) - \frac{2}{3}\sigma^{(3)}(T)k^2\right], \tag{22}$$

causing the anharmonic phase shift of XAFS spectra.

In the anharmonic XAFS function given by Eq. (20), S_0^2 is the square of the many body overlap term, N_j is

the atomic number of each shell, the second cumulant σ^2 and its anharmonic contribution σ_A^2 are calculated by Eqs. (13) and (18), respectively, the mean free path λ is defined by the imaginary part of the complex photoelectron momentum $p = k + i/\lambda$, and the sum j is over all the considered atomic shells.

Hence, the above derived expressions for the first, third cumulants and thermal expansion coefficient $\sigma^{(1)}$, $\sigma^{(3)}$ and α_T, respectively, the total second cumulant given by Eqs. (17) – (19) including anharmonic effects, as well as the XAFS function given by Eqs. (20) – (22) have been presented in terms of second cumulant σ^2 or MSRD. Such description leads to the present advanced method based on that the calculations and measurements are necessary only for the second cumulants from which all the considered XAFS parameters can be provided.

2.2. Experimental

The measurements of second cumulants or MSRDs of Zn in hcp phase at 300 K, 400 K, 500 K and 600 K and XAFS spectra at these temperatures have been performed at the Beamline BL8, SLRI (Thailand). It is the routinely operated for X-ray absorption spectroscopy (XAS) in an immediate photon energy range (1.25 – 10 keV). The experimental set-up conveniently facilitates XAS measurements in transmission and fluorescence-yield modes at several K-edges of elements ranging from Magnesium to Zinc [12]. The experimental values of the first, third cumulants, and thermal expansion coefficients of Zn at 300 K, 400 K, 500 K, 600 K have been extracted from the measured values of the second cumulants using the present advanced method presented in Section 2.1. The obtained experimental results are presented in Section 3 compared to the calculated results and to those measured in HASYLAB (DESY, Germany) at 77 K and 300 K [10].

3. NUMERICAL RESULTS COMPARED TO EXPERIMENT AND DISCUSSIONS

Now the expressions derived in the Section 2.1 are applied to numerical calculations for Zn in hcp phase using its Morse potential parameters [13] D = 0.1700 eV, α = 1.7054 $Å^{-1}$ which were obtained using experimental values for the energy of sublimation, the compressibility, and the lattice constant.

Figure **1** illustrates good agreement of first cumulant $\sigma^{(1)}(T)$ of Zn calculated using the present theory with the experimental values at 300 K, 400 K, 500 K, and 600 K extracted using the present advanced method and with those measured in HASYLAB (DESY, Germany) at 77 K and 300 K [10]. Note that using the first cumulant the temperature dependence of near atomic neighbor distance can be obtained based on the expression $R(T) = R(0) + \sigma^{(1)}(T)$.

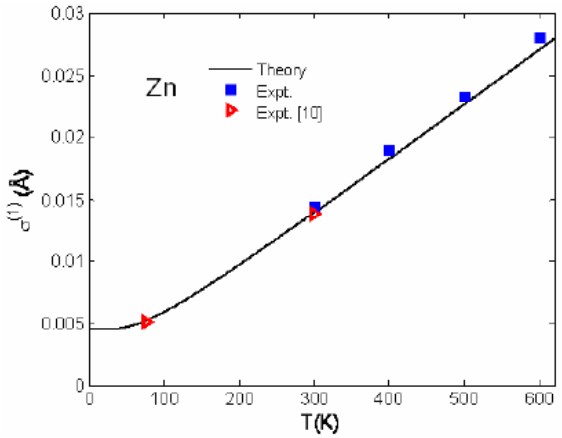

Figure 1: Temperature dependence of first cumulant $\sigma^{(1)}(T)$ of Zn calculated using the present theory compared to the experimental values at 300 K, 400 K, 500 K and 600 K extracted using the present advanced method and with those measured in HASYLAB (DESY, Germany) at 77 K and 300 K [10].

The good agreement of total and harmonic second cumulants $\sigma_{tot}^2(T)$, $\sigma^2(T)$, respectively, of Zn calculated using the present theory with the experimental values at 300 K, 400 K, 500 K, 600 K obtained in this work and with those measured in HASYLAB (DESY, Germany) at 77 K and 300 K [10] is presented in Figure **2**. Here, $\sigma_{tot}^2(T)$ is a little different from $\sigma^2(T)$ at temperatures greater than the room temperature due to the anharmonic contributions.

Figure **3** shows good agreement of temperature dependence of third cumulant $\sigma^{(3)}(T)$ of Zn calculated using the present theory with the experimental values at 300 K, 400 K, 500 K, 600 K extracted using the present advanced method and with those measured in HASYLAB (DESY, Germany) at 77 K and 300 K [10].

Note that the obtained first cumulant (Figure **1**) and second cumulant (Figure **2**) are linearly proportional to the temperature T and the third cumulant to T^2 at high-temperatures, and all they contain zero-point energy contributions at low-temperatures, a quantum effect, as for the other crystal structures [9].

Temperature dependence of thermal expansion coefficient $\alpha_T(T)$ of Zn calculated using the present

theory (Figure **4**) agrees well with the experimental values at 300 K, 400 K, 500 K, 600 K extracted using the present method and with those measured in HASYLAB (DESY, Germany) at 77 K and 300 K [10]. Here, the theoretical and experimental thermal expansion coefficients of Zn approach the constant values at high-temperatures as it was obtained for the other crystal structures [9].

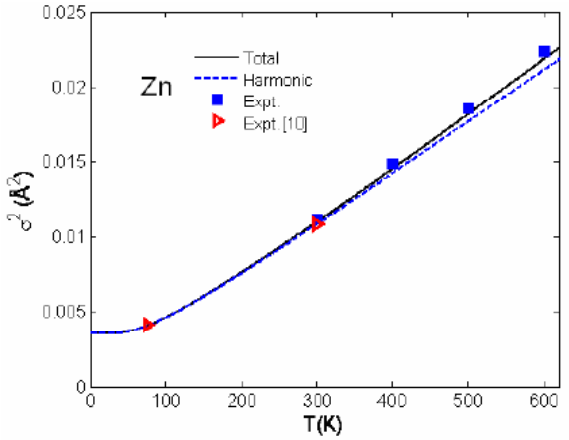

Figure 2: Temperature dependence of total and harmonic second cumulants $\sigma^2_{tot}(T)$ and $\sigma^2(T)$, respectively, of Zn calculated using the present theory compared to the experimental values at 300 K, 400 K, 500 K and 600 K obtained in this work and with those measured in HASYLAB (DESY, Germany) at 77 K and 300 K [10].

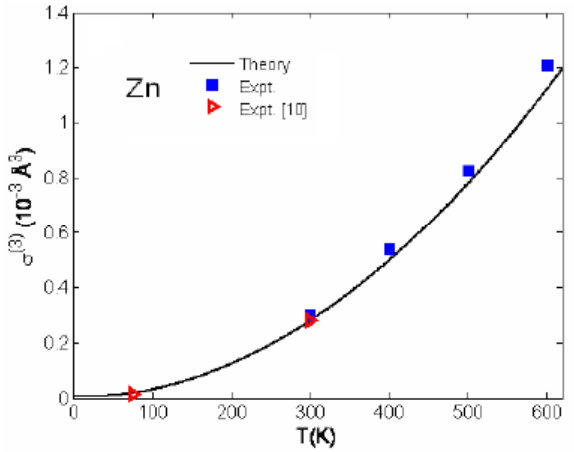

Figure 3: Temperature dependence of third cumulant $\sigma^{(3)}(T)$ of Zn calculated using the present theory compared to the experimental values at 300 K, 400 K, 500 K, 600 K extracted using the present advanced method and to those measured in HASYLAB (DESY, Germany) at 77 K and 300 K [10].

Note that the second cumulant describing MSRD is primary a harmonic effect plus small anharmonic contributions which appear only at high-temperatures. But the first cumulant describing the net thermal expansion or lattice disorder, the third cumulant or MCRD describing the asymmetry of pair atomic distribution function and the thermal expansion coefficient are entirely anharmonic effects because they appear due to including the cubic anharmonic effective potential parameter. Consequently, the obtained theoretical and experimental XAFS cumulants and thermal expansion coefficients describe apparently the thermodynamic properties and anharmonic effects of hcp crystals. They show the good agreement not only between the theoretical and experimental results calculated and extracted by using the present advanced method but also of their good agreement with those measured at HASYLAB (DESY, Germany) [10].

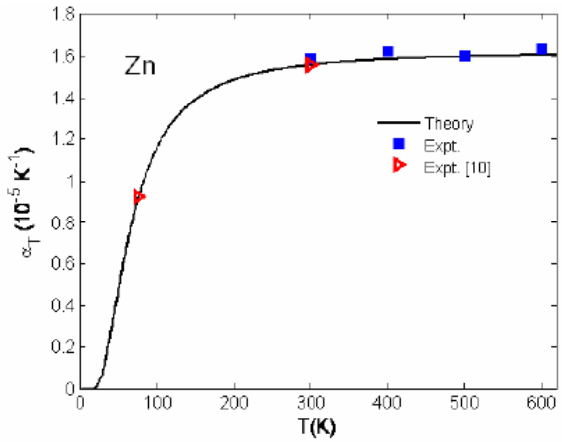

Figure 4: Temperature dependence of thermal expansion coefficient $\alpha_T(T)$ of Zn calculated using the present theory compared to the experimental values at 300 K, 400 K, 500 K, 600 K extracted using the present method and to those measured in HASYLAB (DESY, Germany) at 77 K and 300 K [10].

For calculating the anharmonic XAFS spectra and their Fourier transform magnitudes of Zn the FEFF code [15] has been modified by including the above cumulants calculated using the present theory. Figure **5** illustrates good agreement of XAFS spectra of Zn at 300 K, 400 K, 500 K and 600 K calculated using the present theory with their experimental data measured at the Beamline BL8, SLRI (Thailand). Here, the anharmonic amplitude attenuation and phase shift are evidently shown in both the theoretical and experimental XAFS spectra as the k-value and temperature T increases.

The above theoretical and experimental anharmonic XAFS spectra have been Fourier transformed and their Fourier transform magnitudes are presented in

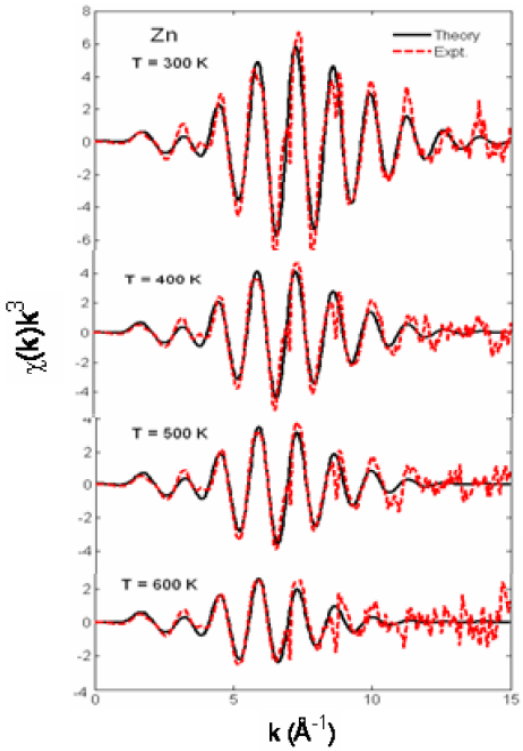

Figure 5: Comparison of anharmonic XAFS spectra of Zn at 300 K, 400 K, 500 K and 600 K of Zn calculated using the present theory with their experimental data measured at the Beamline BL8, SLRI (Thailand).

Figure **6**. They show good agreement between the theoretical and experimental results, as well as the decrease of peak heights and their shifts to the left as the temperature T increases.

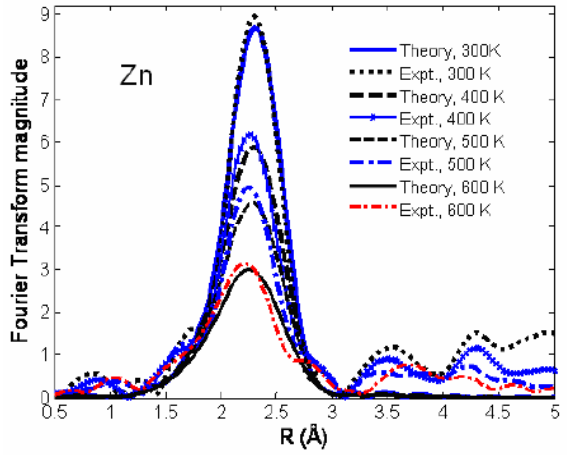

Figure 6: Comparison of Fourier transform magnitudes of theoretical and experimental XAFS spectra of Zn at 300 K, 400 K, 500 K and 600 K presented in Figure **5**.

CONCLUSIONS

In this work, the thermodynamic properties, anharmonic effects and structural determination of hcp crystals have been studied based on the theoretical and experimental DWFs presented in terms of cumulant expansion and thermal expansion coefficient, as well as XAFS spectra and their Fourier transform magnitudes.

The most advantageous development in this work is the advanced method derived based on quantum statistical theory using which all the considered theoretical and experimental XAFS quantities have been calculated or extracted from the calculated or measured second cumulants or MSRDs. This leads to significant simplification and reduction of XAFS calculations and measurements.

The obtained temperature-dependent theoretical and experimental XAFS quantities have been in detail analyzed and valuated. They include the evident anharmonic effects and satisfy all their fundamental properties, as well as reach the classical values at high-temperatures and contain zero-point energy contributions at low-temperatures, a quantum effect.

The good agreement between the theoretical results calculated using the present theory and the experimental data extracted using the present advanced method, as well as their good agreement with those measured in HASYLAB (DESY, Germany) for Zn illustrate the simplicity and efficiency of the present derived method in XAFS data analysis and in materials studies.

REFERENCES

[1] Crozier ED, Rehr JJ and Ingalls R. in X-ray Absorption, edited by DC. Koningsberger and R. Prins (Wiley, New York, 1988). Chap. 9.

[2] Tranquada JM and Ingalls R. Extended x-ray-absorption fine-structure study of anharmonicity of CuBr, Phys Rev 1983; B 28: 3520.

[3] Fernando D. Vila, Rehr JJ, Rossner HH and Krappe HJ. Theoretical x-ray absorption Debye-Waller factors, Phys Rev 2007; B 76: 014301.

[4] Hung NV, Hung VV, Hieu HK, Frahm RR. Pressure effects in Debye-Waller factors and in EXAFS, Phys 2011; B 406: 456.

[5] Hung NV, Thang CS, Toan NC, Hieu HK. Temperature dependence of Debye-Waller factors of semiconductors, VAC 2014; 101: 63. https://doi.org/10.1016/j.vacuum.2013.07.021

[6] Hung NV. Pressure-dependent anharmonic correlated Einstein model XAFS Debye-Waller factors, J Phys Soc Jpn 2014; 83: 024802. https://doi.org/10.7566/JPSJ.83.024802

[7] Hung NV, Tien TS, Duc NB, Vuong DQ. High-order expanded XAFS Debye-Waller factors of hcp crystals based on classical Anharmonic correlated Einstein model, Mod Phys Lett 2014; B 28: 1450174.

[8] Hung NV, Hue TT, Khoa HD, Vuong DQ. Anharmonic correlated Debye model high-order expanded interatomic

effective potential and Debye-Waller factor of bcc crystals, Phys 2016; B 503: 174-178.

[9] Hung NV and Rehr JJ. Anharmonic correlated Einstein model Debye-Waller factors, Phys Rev 1997; B 56: 43.

[10] Hung NV, Tien TS, Hung LH, Frahm RR. Anharmonic Effective Potential, Local Force Constant and EXAFS of HCP Crystals: Theory and Comparison to Experiment, Int J Mod Phys 2008; B 22: 5155.

[11] Feynman RP. Statistical Mechanics, edited by Jacob Shaham, WA. Benjamin, INC. Advanced book Program, Reading, Massachusetts 1972.

[12] Klysubun W, Sombunchoo P, Deenam W, Komark C. Performance and status of beamline BL18 at SLRI for X-ray absorption spectroscopy, J Synchrotron Rad 2012; 19: 930. https://doi.org/10.1107/S0909049512040381

[13] Hung NV. A method for calculation of Morse potential for fcc, bcc, hcp crystals applied to Debye-Waller factors and equation of state, Commu. in Phys (CIP) 2004; 14(1): 7-14.

[14] Hung NV, Duc NB, Frahm RR. A new anharmonic factor and EXAFS including anharmonic contributions, J Phys Soc Jpn 2003; 72: 1254. https://doi.org/10.1143/JPSJ.72.1254

[15] Rehr JJ, Mustre de Leon J, Zabinsky SI, Albers RC. Theoretical X-ray Absorption Fine Structure Standards, J Am Chem Soc 1991; 113: 5135. https://doi.org/10.1021/ja00014a001

Received on 02-12-2017 Accepted on 22-12-2017 Published on 09-01-2018

http://dx.doi.org/10.15379/2408-977X.2017.04.02.02